Seed run-off in an MHD air preheater
by Rosanne Marie Nash

A thesis submitted in partial fulfillment of the requirements for the degree of MASTER OF SCIENCE in MECHANICAL ENGINEERING
Montana State University

Abstract:
Potassium sulphate (seed) flow and buildup on a tube wall of a cored brick regenerative air preheater was modeled using an adaptation of a previously developed slag flow computer model. The slag and seed flow problems will be encountered in air preheaters used in proposed open cycle magnetohydrodynamic (MHD) power generation. Two cases of flow which simulated experimental conditions of two runs on the Flui-Dyne Engineering Corporation experimental air preheater were modeled. Comparison of analytical and experimental results showed that the model can reasonably predict the occurrence of flow restrictions in the tube due to seed buildup but the magnitudes of the restrictions cannot be predicted due to limitations of the model.

STATEMENT OF PERMISSION TO COPY

In presenting this thesis in partial fulfillment of the requirements for an advanced degree at Montana State University, I agree that the Library shall make it freely available for inspection. I further agree that permission for extensive copying of this thesis for scholarly purposes may be granted by my major professor, or, in his absence, by the Director of Libraries. It is understood that any copying or publication of this thesis for financial gain shall not be allowed without my written permission.

Signature Rosanne M. Nash

Date 10/2/78

SEED RUN-OFF IN AN MHD AIR PREHEATER

by

ROSANNE MARIE NASH

A thesis submitted in partial fulfillment
of the requirements for the degree

of

MASTER OF SCIENCE

in

MECHANICAL ENGINEERING

Approved:

H. W. Tuttle
Chairperson, Graduate Committee

Dennis O. Blackketter
Head, Major Department

Henry L Parsons
Graduate Dean

MONTANA STATE UNIVERSITY
Bozeman, Montana

October, 1978

ACKNOWLEDGEMENTS

The author would like to thank Dr. H. W. Townes for his help and guidance in preparing this thesis. The author would also like to thank her husband, Rusty, for his support and encouragement.

TABLE OF CONTENTS

LIST OF TABLES

LIST OF FIGURES

NOMENCLATURE

Symbol	Description
A	Cross-sectional area of flow
BT	Total blowdown cycle time
c	Fluid specific heat
C	Circumference of flow tube
C_+	Weight concentration of seed in gas stream
D	Diameter of flow tube
f	Friction factor
g	Acceleration due to gravity
k	Fluid thermal conductivity
k_s	Equivalent sand grain roughness factor
k_+	Dimensionless particle deposition velocity
L	Length of axial element
$\dot{m}$	Seed mass deposition from gas stream
$\dot{m}_a$	Mass flow rate of gas stream
P	Local pressure
r	Radial position
Re	Reynolds number for gas flow
RT	Total reheat cycle time
t	Time
T	Fluid temperature
Temp	Wall temperature

Symbol	Description
TK	Gas stream temperature
u	Velocity component in axial direction
v	Velocity component in radial direction
V	Average gas velocity
$\overline{V}$	Mean fluid velocity
$\forall$	Elemental volume
$\dot{\forall}$	Volumetric flow rate
y	Dimension measured from tube wall inward
Z	Axial position
Δt	Time step
ΔZ	Axial step
δ	Fluid layer thickness
ρ	Fluid density
ρ_f	Gas stream density
μ	Dynamic viscosity
τ_g	Surface shear due to gas flow

subscript j denotes axial step

superscript n denotes time step

ABSTRACT

Potassium sulphate (seed) flow and buildup on a tube wall of a cored brick regenerative air preheater was modeled using an adaptation of a previously developed slag flow computer model. The slag and seed flow problems will be encountered in air preheaters used in proposed open cycle magnetohydrodynamic (MHD) power generation. Two cases of flow which simulated experimental conditions of two runs on the Flui-Dyne Engineering Corporation experimental air preheater were modeled. Comparison of analytical and experimental results showed that the model can reasonably predict the occurrence of flow restrictions in the tube due to seed buildup but the magnitudes of the restrictions cannot be predicted due to limitations of the model.

CHAPTER I

INTRODUCTION

Efficient operation of proposed coal-fired, open-cycle magnetohydrodynamic (MHD) power generating plants will require combustion gas temperatures on the order of 3000°K. A prerequisite for successfully obtaining these temperatures is that the combustion air be preheated prior to the combustion process.

A ceramic fixed-bed regenerative heat exchanger utilizing exhaust gases from the MHD channel to preheat incoming combustion air is currently being considered. A major problem associated with this system involves the corrosive potassium sulphate seed- and coal slag-laden MHD exhaust gases. As the gases cool during the heat up of the heat exchanger matrix, the seed and slag particles will condense and deposit along the ceramic walls. The resulting behavior of the seed/slag layer with respect to flow and growth could be a determining factor in the feasibility of the regenerative heat exchanger system.

Consequently, a significant amount of experimental and analytical research has been carried out in an effort to determine the characteristics of the seed/slag flow. An analytical computer model was developed at Montana State University [Clowes, 1] to predict slag flow and build up on the experimental facility located there. The objective of this thesis has been to adapt that analytical slag flow model to the conditions of the FluiDyne Engineering Corporation experimental heat exchanger and to compare these analytical results with the experimental

results obtained by FluiDyne. The FluiDyne facility tested primarily seed flow and the possibility of using pressure drop measurements as an indicator of seed/slag buildup on passage walls.

CHAPTER II

LITERATURE REVIEW

Before seed flow in an MHD air preheater can be adequately modeled, the seed mass deposition rate from the gas stream to the passage walls must be accurately known. Many analytical and experimental studies have attempted to determine the rate of particulate deposition from turbulent flow streams. General theoretical models have been developed by Friedlander and Johnstone [2], Davies [3], and Sande [4]. Experimental studies were done by Friedlander and Johnstone [2], and Liu and Agarwal [5]. Ondo [6] reviewed several of the theoretical models and experimental studies. Ondo's review showed that the theoretical models agreed with experimental results for only limited ranges of deposition rates. Overall, the experimental results had a two-order-of-magnitude variation and the theoretical models had a four-order-of-magnitude variation. This indicates that more theoretical and experimental work needs to be done before seed deposition in an MHD air preheater can be accurately predicted.

Slag flow in an MHD channel has been theoretically modeled by Rosa [7]. Experimental measurements of slag flow and slag properties in a simulated MHD channel have been carried out by Rodgers, Ariessohn and Kruger [8].

Clowes [1] developed a theoretical model for slag flow in an MHD air preheater. In the present work, this model has been modified and used to predict seed flow in an MHD air preheater.

CHAPTER III

THEORY

The matrix of a ceramic fixed-bed air preheater consists of a stack of cored bricks which form an array of cylindrical flow passages A model of the seed flow in a single passage is sufficient as the results may be extended to any number of passages provided they are all operating under the same flow conditions.

The momentum, energy, and continuity equations governing the axi-symmetric flow of a layer of constant density fluid down the inside of a vertically oriented cylinder from Clowes [1] are as follows:

Momentum:

$$\rho\left(\frac{\partial u}{\partial t} + u\frac{\partial u}{\partial z} + v\frac{\partial u}{\partial r}\right) = \rho g - \frac{\partial P}{\partial z} + \mu\left(\frac{\partial^2 u}{\partial z^2} + \frac{1}{r}\frac{\partial u}{\partial r} + \frac{\partial^2 u}{\partial r^2}\right) + \frac{\partial \mu}{\partial r}\left(\frac{\partial v}{\partial z} + \frac{\partial u}{\partial r}\right) + 2\frac{\partial u}{\partial z}\frac{\partial \mu}{\partial z} \tag{1}$$

where ρ = fluid density,

u = velocity component in axial direction,

v = velocity component in radial direction,

μ = dynamic viscosity,

g = acceleration due to gravity,

r = radial position,

z = axial position,

P = local pressure, and

t = time.

Energy: (with negligible shear work)

$$\frac{\partial}{\partial z}(u\rho cT) + \frac{1}{r}\frac{\partial}{\partial r}(rvc\rho T) - \frac{\partial}{\partial z}\left(k\frac{\partial T}{\partial z}\right) - \frac{1}{r}\frac{\partial}{\partial r}\left(rk\frac{\partial T}{\partial r}\right) + \rho c\frac{\partial T}{\partial t} = 0 \quad (2)$$

where T = fluid temperature,

c = fluid specific heat, and

k = fluid thermal conductivity.

Continuity:

$$\rho\frac{\partial \forall}{\partial t} = \rho\dot{\forall}_{in} - \rho\dot{\forall}_{out} \quad (3)$$

where $\forall$ = volume, and

$\dot{\forall}$ = volumetric flow rate.

Clowes [1] determined that the stability criteria limiting the size of axial and time steps are too severe to allow a workable solution of the three coupled equations.

In order to obtain a workable model of slag or seed flow, an additional limitation must be imposed. By constraining the model to apply to a thin fluid layer, the temperature can be considered to be constant radially and equal to the ceramic wall temperature [Clowes, 1]. If the axial temperature variation of the wall is known, the energy equation is no longer needed. Since the viscosity is temperature dependent, it, also, will vary only with axial position.

Using these simplifications and rectangular coordinates, the momentum equation at any one axial position becomes the following relationship for the radial velocity profile [Clowes, 1]:

$$u(y) = \frac{-\rho g}{2\mu_j} y^2 + \frac{(\tau_g)_j + \rho g \delta_j}{\mu_j} y \qquad (4)$$

where j = axial position of calculation,

τ_g = surface shear stress due to gas flow,

δ = fluid layer thickness, and

y = dimension measured from the tube wall inward.

In the same way, the expanded continuity equation becomes the following partial differential equation (see Appendix 1 for development):

$$\frac{\dot{m}}{\rho} + \frac{\partial(\delta \overline{V})}{\partial z} = \frac{\partial \delta}{\partial t} \qquad (5)$$

where $\dot{m}$ = seed mass deposition from gas stream,

$\overline{V}$ = seed mean fluid velocity,

$$= \frac{1}{\delta} \int_o^\delta u(y)\, dy, \text{ and}$$

$$= \frac{\tau_g \delta}{2\mu} + \frac{\rho_g \delta^2}{3\mu}.$$

Equation 5 can be solved using a backward finite difference with respect to fluid velocity direction (see Appendix 1 for explanation). For fluid flowing down the bed with the zero axial position at the top of the bed, equation 5 is approximated as:

$$\delta_j^{n+1} = \delta_j^n + \Delta t \frac{\dot{m}_j}{\rho} + \frac{\Delta t}{\Delta z}\left(\delta_{j-1}^n \cdot \overline{V}_{j-1}^n - \delta_j^n \cdot \overline{V}_j^n\right) \qquad (6)$$

where superscript n denotes time, and

subscript j denotes axial position, measured from top of bed.

Solution of the thickness finite difference equation and the corresponding mean velocity equation requires knowledge of the ceramic wall temperature, seed viscosity, surface shear due to the gas flow, and seed mass deposition rate at all axial positions and at all times during the flow simulation.

The axial temperature variation can be either a curve fit of experimentally measured values or a curve fit of values calculated with an appropriate analytical heat transfer model. If the temperature also varies with time, the functional dependence with respect to time may be fitted in a similar manner.

The seed viscosity is a function of temperature for which empirical relationships are available.

The surface shear due to gas flow can be approximated using the following rough regime pressure drop relationship, the Colebrook-White friction factor relationship, and the shear stress equation:

$$\frac{P_1}{\rho_1 g} + Z_1 = \frac{P_2}{\rho_2 g} + Z_2 + f \frac{L}{D} \frac{V^2}{2g} \qquad (7)$$

where P = local pressure,

Z = axial position,

γ = specific weight of the gas,

f = friction factor,

L = length of axial element,

D = diameter of flow passage,

V = average gas velocity, and

ρ = gas density.

$$\frac{1}{\sqrt{f}} = 1.74 - 2 \log_{10} \left[\frac{2 k_s}{D} + \frac{18.7}{Re\sqrt{f}} \right] \tag{8}$$

where k_s = equivalent sand grain roughness factor, and

Re = Reynold's number for gas flow;

$$\tau = \frac{f}{4} \frac{\rho_f V^2}{2 g_c} \tag{9}$$

where ρ_f = gas stream density.

These equations can be solved at different times at each axial element and the resulting shear values can be fitted to give a relationship for shear variation with axial position and time. Either the total pressure drop across the bed or the equivalent sand grain roughness factor must be a known parameter. This development agrees with a thin seed layer approximation in that it does not take into account possible gas flow variations due to a thick seed layer buildup.

The rate at which seed is being deposited onto the flow passage wall is not an easily measured or calculated value. The experimental work of Liu and Agarwal [5] parallels the conditions of an MHD air preheater better than most of the other experimental deposition studies. Their results also agree well with theoretical models over the middle range of deposition velocities as shown by Ondo [6]. Therefore, a first order approximation of seed mass deposition rate can be made by using an experimental deposition velocity from Liu and Agarwal [5] and considering it not to vary with axial position or time.

The seed thickness can now be determined by dividing the air preheater bed into a number of axial steps and calculating the corresponding thickness and mean velocity at each axial position for one time. Time is then incremented by one step and the axial calculations repeated.

CHAPTER IV

RESULTS

Two cases of seed flow were modeled. The flow conditions for the two cases correspond to those encountered in FluiDyne's experimental test 5, listed in Tables 1 and 2. This data was obtained from White [9] and Pearson [10] and was used to develop functional forms of the variations of wall temperature, seed viscosity, shear stress due to gas flow, and seed mass deposition rates (see Appendix 2 for details).

The two test cases are designated as stable and unstable. The stable experimental run showed no change in the pressure drop across the bed with an increasing number of cycles while the unstable experimental run showed an increasing pressure drop across the bed with increasing number of cycles. The air preheater bed was found to have significant seed deposition within its flow passages after the unstable experimental run. For both cases the tube diameter was 19.1 mm and the tube length (bed length) was 5.182 m. The seed material used was potassium sulphate.

The term "reheat" refers to the air preheater operational phase in which the bed is being heated by the hot exhaust gases. The term "blowdown" refers to the operational phase in which the precombustion air is being heated by the hot bed. A "cycle" is a combined reheat and blowdown phase.

TABLE 1.--Stable Case Flow Conditions

Bed Geometry:

Bed Length = 5.182 m

Number of flow holes = 30

Diameter of flow holes = 19.1 mm

Flow Times:

Reheat cycle time = 60 min.

Blowdown cycle time = 30 min.

Total run time = 30 hr. 35 min.

Number of cycles = 20

Reheat Cycle:

Total gas mass flow rate = 0.0998 kg/sec

Inlet weight concentration of seed in gas = 2.53%

Maximum top temperature = 1846°K

Maximum bottom temperature = 1386°K

Inlet pressure = 103,422 Pa

Pressure drop across the bed = 6216 Pa

Blowdown Cycle:

Total air mass flow rate = 0.1066 kg/sec

Minimum top temperature = 1630°K

Minimum bottom temperature = 1188°K

Inlet pressure = 103,422 Pa

Pressure drop across the bed = 5221 Pa

Seed Material - Potassium Sulphate:

Density = 2660 kg/m^3

Solidification temperature = 1344°K

TABLE 2.--Unstable Case Flow Conditions

Bed Geometry:

Bed length = 5.182 m
Number of flow holes = 30
Diameter of flow holes = 19.1 mm

Flow Times:

Reheat cycle time = 30 min.
Blowdown cycle time = 30 min.
Total run time = 5 hr. 20 min.
Number of cycles = 5

Reheat Cycle:

Total gas mass flow rate = 0.0921 kg/sec
Inlet weight concentration of seed in gas = 2.74%
Maximum top temperature = 1715°K
Maximum bottom temperature = 1289°K
Inlet pressure = 103,422 Pa
Pressure drop across the bed = 6987 → 9523 Pa

Blowdown Cycle:

Total air mass flow rate = 0.0809 kg/sec
Minimum top temperature = 1522°K
Minimum bottom temperature = 1105°K
Inlet pressure = 103,422 Pa
Pressure drop across the bed = 3580 → 4202 Pa

Seed Material - Potassium Sulphate:

Density = 2660 kg/m^3
Solidification temperature = 1344°K

The major difference in the flow conditions between the two cases is the stable case reheat phase of 60 minutes compared to the unstable case reheat phase of 30 minutes. The result of the longer reheat in the stable case is a higher overall maximum wall temperature profile. By the end of the stable case reheat phase the entire bed length has temperatures above 1344°K, which is the solidification temperature for potassium sulphate.

The results of the two case runs of the seed flow model are shown in Figures 2 through 7. All plots are of the seed thickness profile vs. a dimensionless bed length.

Figure 1 shows the seed thickness profile 1200 seconds into the first 3600 second reheat phase of the stable case. The maximum wall layer thickness is 0.252 mm which occurs at a dimensionless axial position of 0.675. This buildup occurs at the point where the wall temperature falls below the solidification temperature of the seed. Above this point, the deposited seed is flowing down the bed and below this point there is no flow as the deposition is considered to be in the solid phase.

Figure 2 again shows the wall layer thickness profile at 1200 seconds into the first 3600 second reheat of the stable case. This plot is on an expanded horizontal scale to show in greater detail the thin seed layers above and below the seed solidification point. The maximum thickness at the point of solidification extends beyond the scale of the

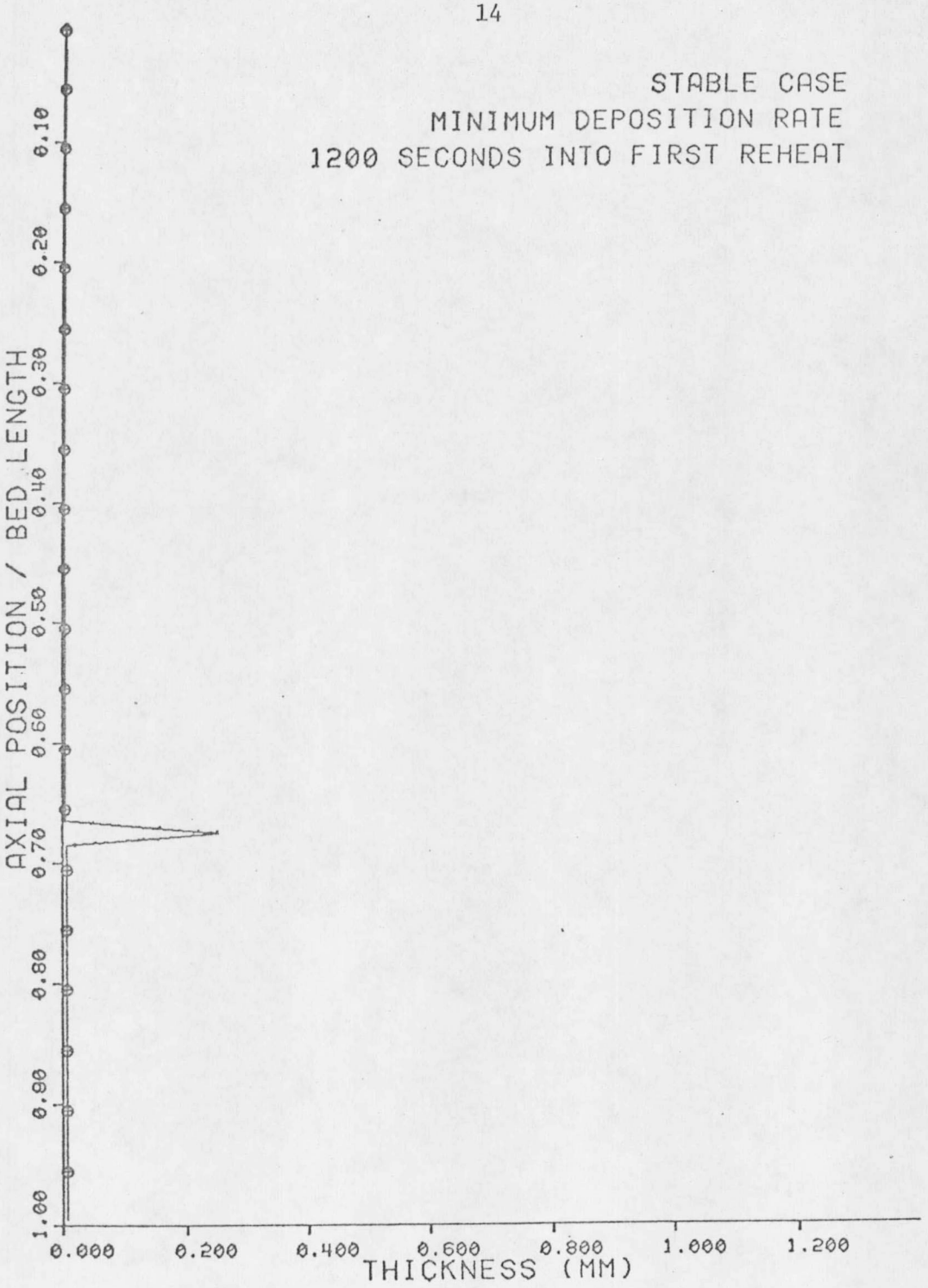

Figure 1.--Seed thickness profile

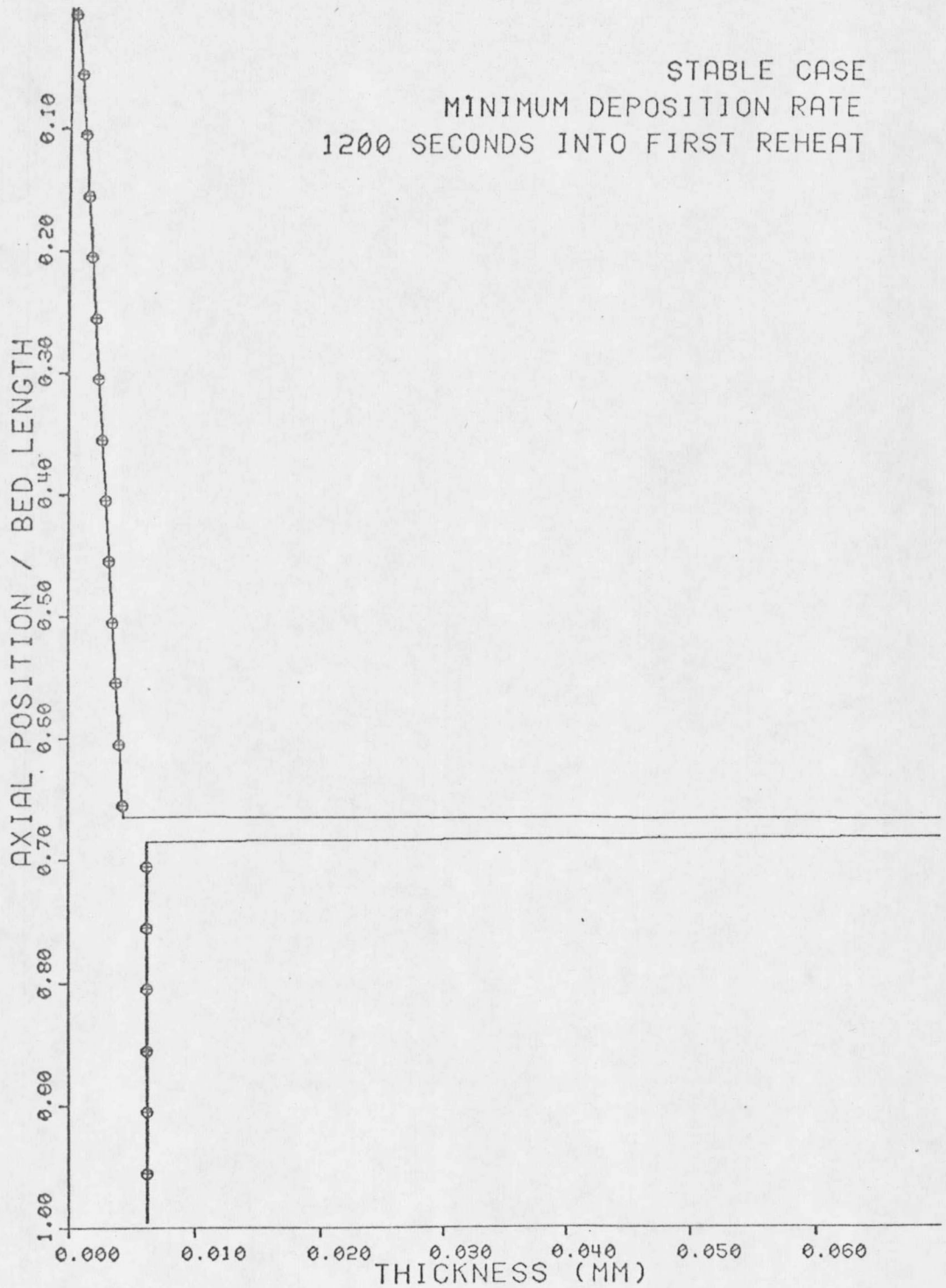

Figure 2.--Seed thickness profile

plot. Above the solidification point, the fluid seed layer has established a very thin equilibrium thickness. Most of the seed that has deposited in this area has flowed down to the point of solidification where the buildup occurs. Below the solidification point there is a almost constant seed thickness. This is due to the constant deposition rate used and zero flow below the solidification temperature.

The plot in Figure 3 shows the seed thickness profile at 2400 seconds into the first reheat phase of the stable case. The maximum thickness is 0.919 mm and occurs at the dimensionless axial position of 0.975. This is the position of the solidification point which has moved down the bed due to continued heat up during the reheat phase. The maximum thickness is increasing with time due to continued deposition and due to the drainage of a larger portion of the bed length.

By 2500 seconds into the reheat cycle the entire bed length has been heated to above the solidification temperature of the seed. Figure 4 shows the seed thickness profile at the end of the reheat phase for cycles one and five. The two profiles coincide which indicates there is cyclic equilibrium. That is, the end of reheat profile does not change because after the first cycle the amount of seed deposited equals the amount of seed that flows out during each cycle. The end of reheat profile for all 20 cycles is the same.

During the blowdown phase of operation, the precombustion gas flow is upward through the air preheater bed. Because the end of reheat seed

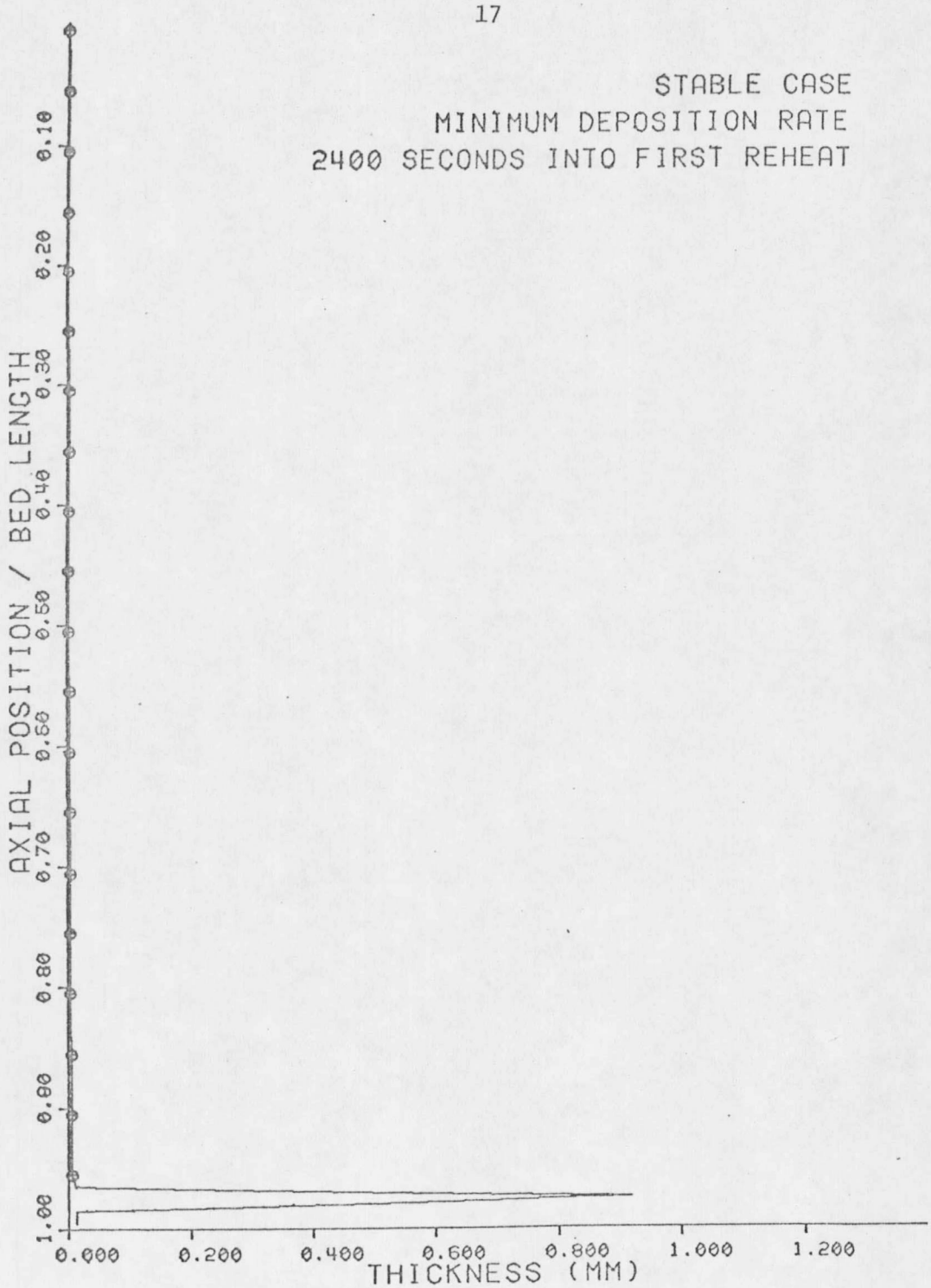

Figure 3.--Seed thickness profile

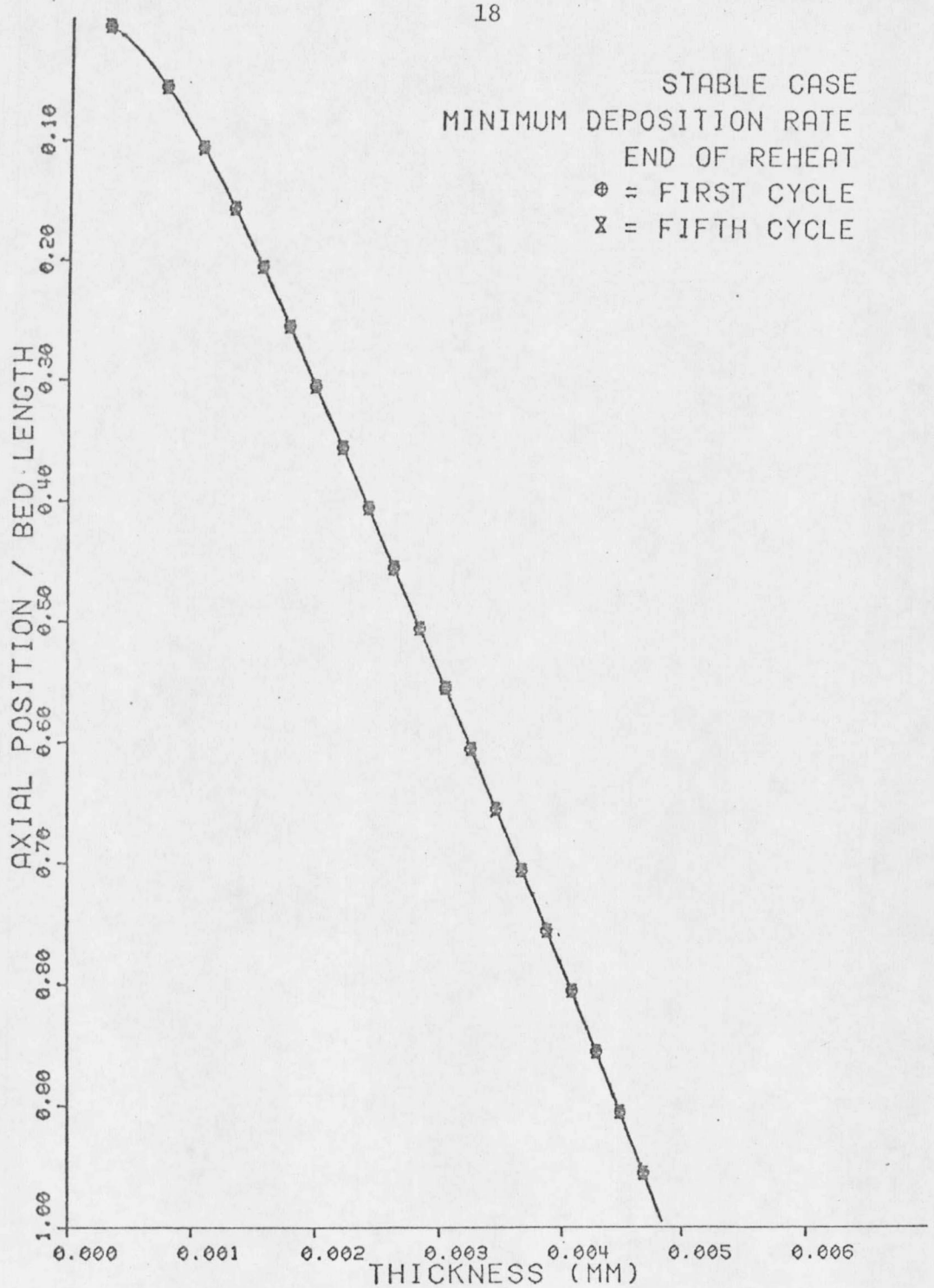

Figure 4.--Seed thickness profile

layer is so thin and the seed viscosity is quite low, the reversal in gas flow direction also causes a reversal in the seed flow direction. Figure 5 shows the seed thickness profile at the end of blowdown for cycles one and five. Again, the two profiles coincide due to cyclic equilibrium. The solidification point is at the dimensionless axial position of 0.46. The steplike decrease in seed thickness at this point is due to the sudden solidification once the wall temperature is below 1344°K. The end of blowdown seed layer thickness is so small that the deposition from the reheat phase can be considered to have completely drained out of the bed by the end of the cycle.

Generally, the seed flow model for the stable case flow conditions has shown that there should be no significant seed buildup on flow passage walls. This agrees with the experimental result of no increase in pressure drop across the bed since there are no flow restrictions to cause an increase.

Figure 6 shows the seed thickness profile at the end of reheat for cycles one and five of the unstable case. The seed solidification temperature occurs at the dimensionless axial position 0.81 for the end of reheat temperature profile. The maximum thickness occurs at the solidification point and is 0.508 mm for the first cycle and 2.36 mm for the fifth cycle. This point of maximum thickness experienced approximately equal growth with each of the 5 cycles. The fluid layer above the solidification point has attained cyclic equilibrium. The solid

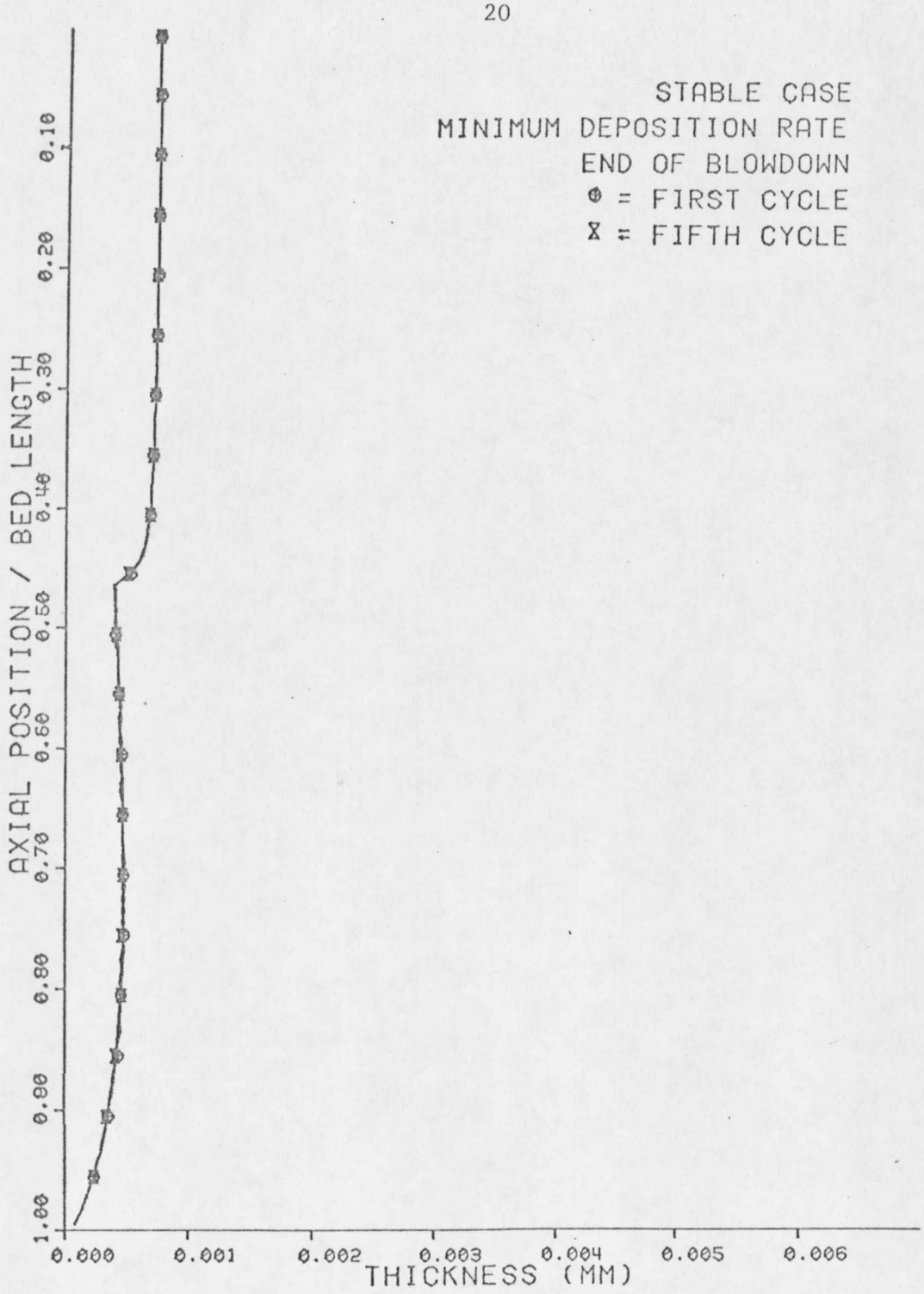

Figure 5.--Seed thickness profile

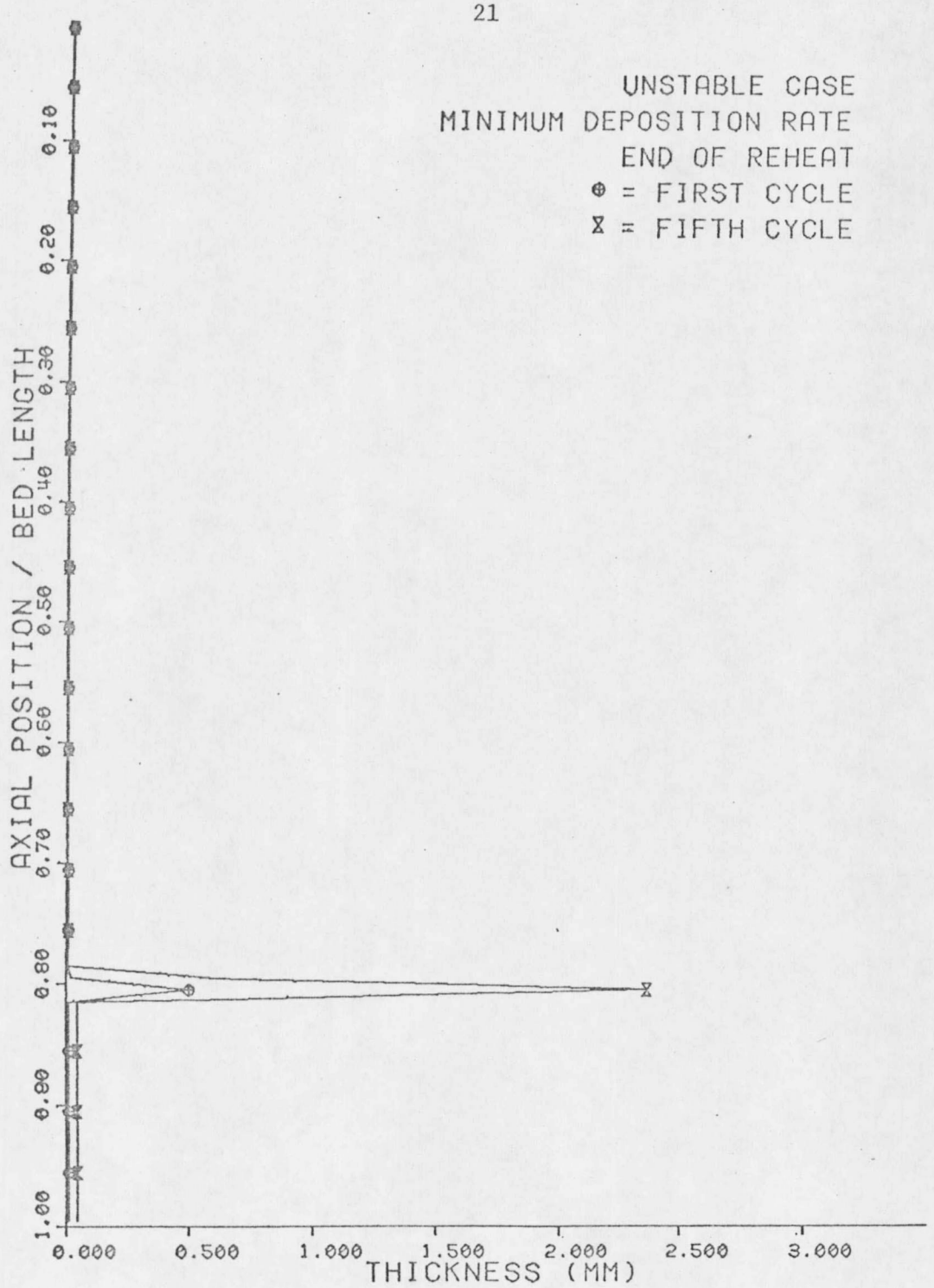

Figure 6.--Seed thickness profile

layer below the solidification point shows growth during the five cycles due to continued deposition.

The end of blowdown seed layer profiles for the first and fifth cycles of the unstable case are shown in Figure 7. The difference between the end of reheat and end of blowdown profiles for the unstable case is that the fluid layer in blowdown is flowing upward and becoming thinner and the solidification point has moved up to the axial position 0.33

The seed flow model for the unstable case has shown that an increasing pressure drop across the bed with increasing number of cycles is to be expected due to a growing flow restriction in the tube. After the fifth cycle the model shows a 43 percent reduction in flow area at the point of maximum seed thickness. A flow reduction of this magnitude exceeds the thin seed layer limitation of the model. Therefore, the actual shape and magnitude of the restriction is not accurately being predicted by the model. In reality, once the seed layer begins to thicken at the point of solidification, a radial temperature gradient will exist and the seed will solidify in a more rounded profile than is indicated by this model. However, the model is accurately predicting the existence of a flow restriction. The model also should be reasonably accurate in predicting the location of the restriction.

Since using a minimum deposition rate from the work of Liu and Agarwal [5] was somewhat arbitrary, both cases were modeled again using

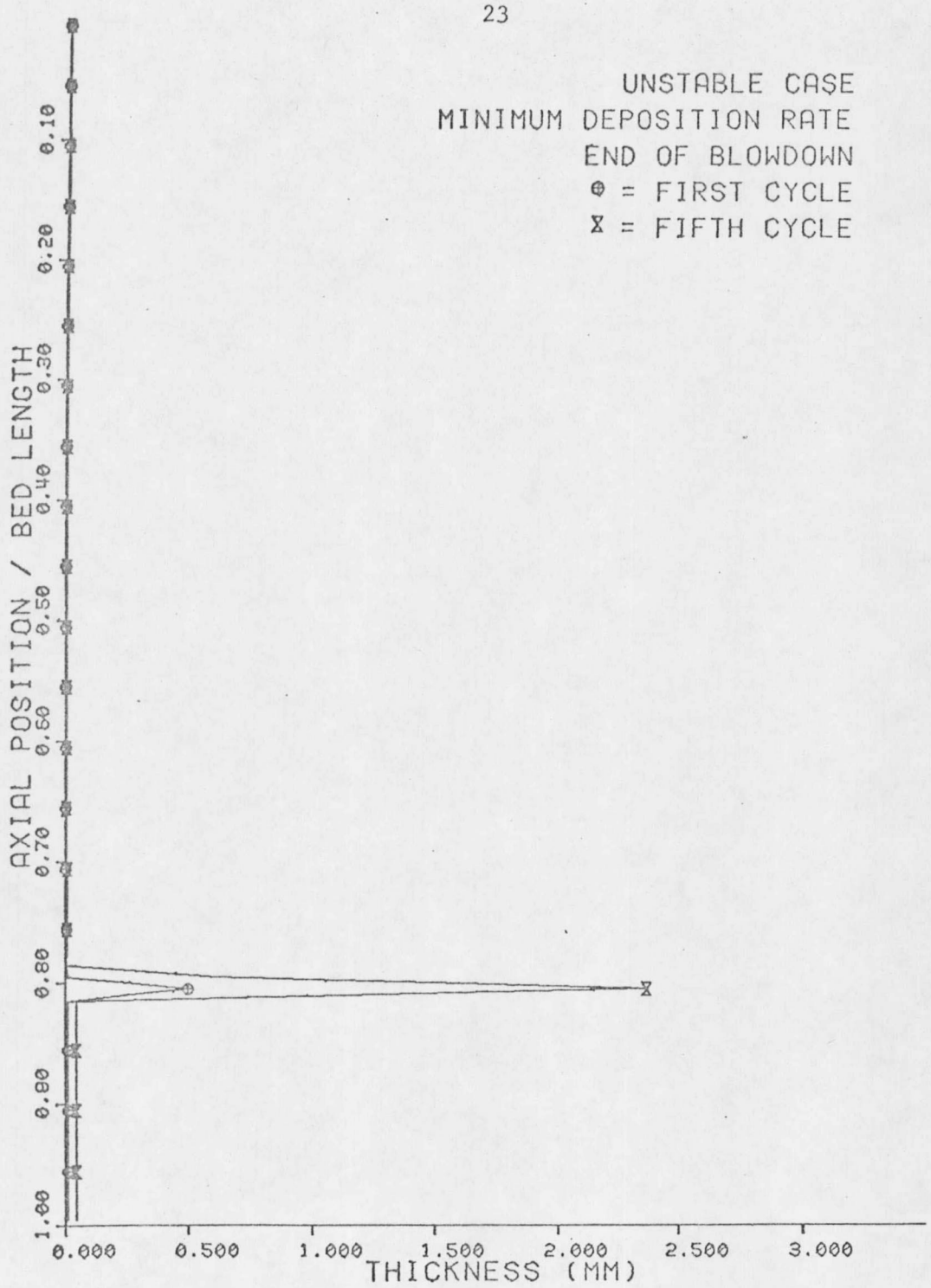

Figure 7.--Seed thickness profile

twice this minimum value to determine the effect of the actual magnitude of deposition rate on the model results. Figures 8, 9, and 10 are seed thickness profiles resulting from the higher deposition rates. The general profile shapes are the same as before but the magnitudes of the maximum seed thickness values are significantly larger. At 2400 seconds into the first reheat of the stable case the maximum thickness is 2.03 mm as compared to the 0.919 mm obtained using the minimum rate. The stable case end of reheat profile is slightly thicker than that obtained with the minimum deposition. This indicates that the equilibrium fluid layer grows slightly with higher deposition rates but most of the additional deposition flows into the solidification point.

The unstable case maximum thicknesses were 1.16 mm at the first end of reheat and 5.17 mm at the fifth end of reheat for the higher deposition rate. Consider the 5.17 mm maximum seed layer thickness to act as an orifice of 8.76 mm diameter. The calculated pressure drop across the bed due to friction and the orifice is 9900 Pa. This is reasonably close to the experimentally measured 9523 Pa pressure drop. However, the similarly calculated pressure drop for the 1.16 mm maximum thickness at the end of the first reheat is not comparable to the measured value of 6987 Pa.

The measured 6987 Pa pressure drop indicates the maximum seed layer thickness at the end of the first reheat of the unstable case should be approximately 4 mm. A seed deposition rate of six times the original

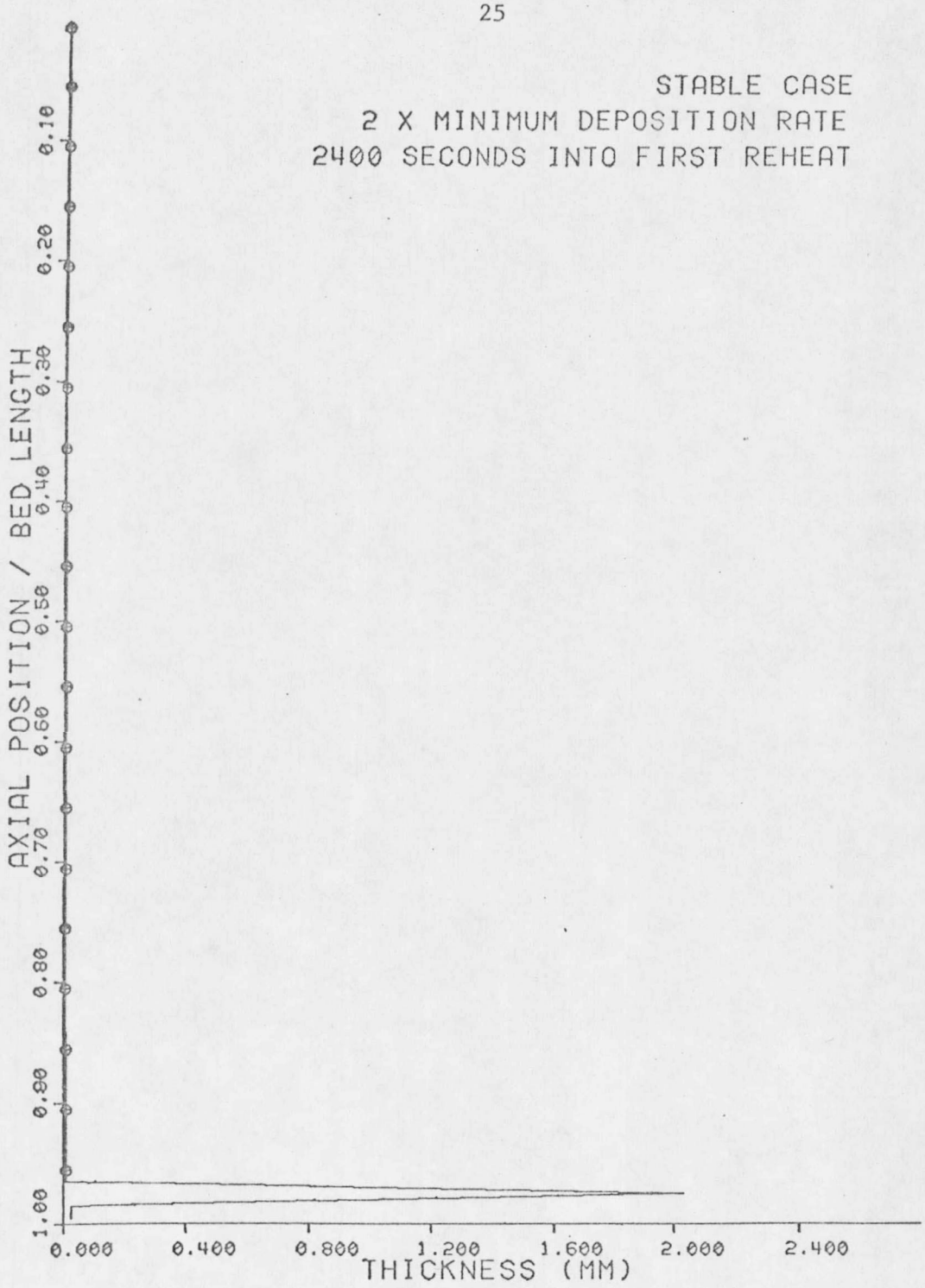

Figure 8.--Seed thickness profile

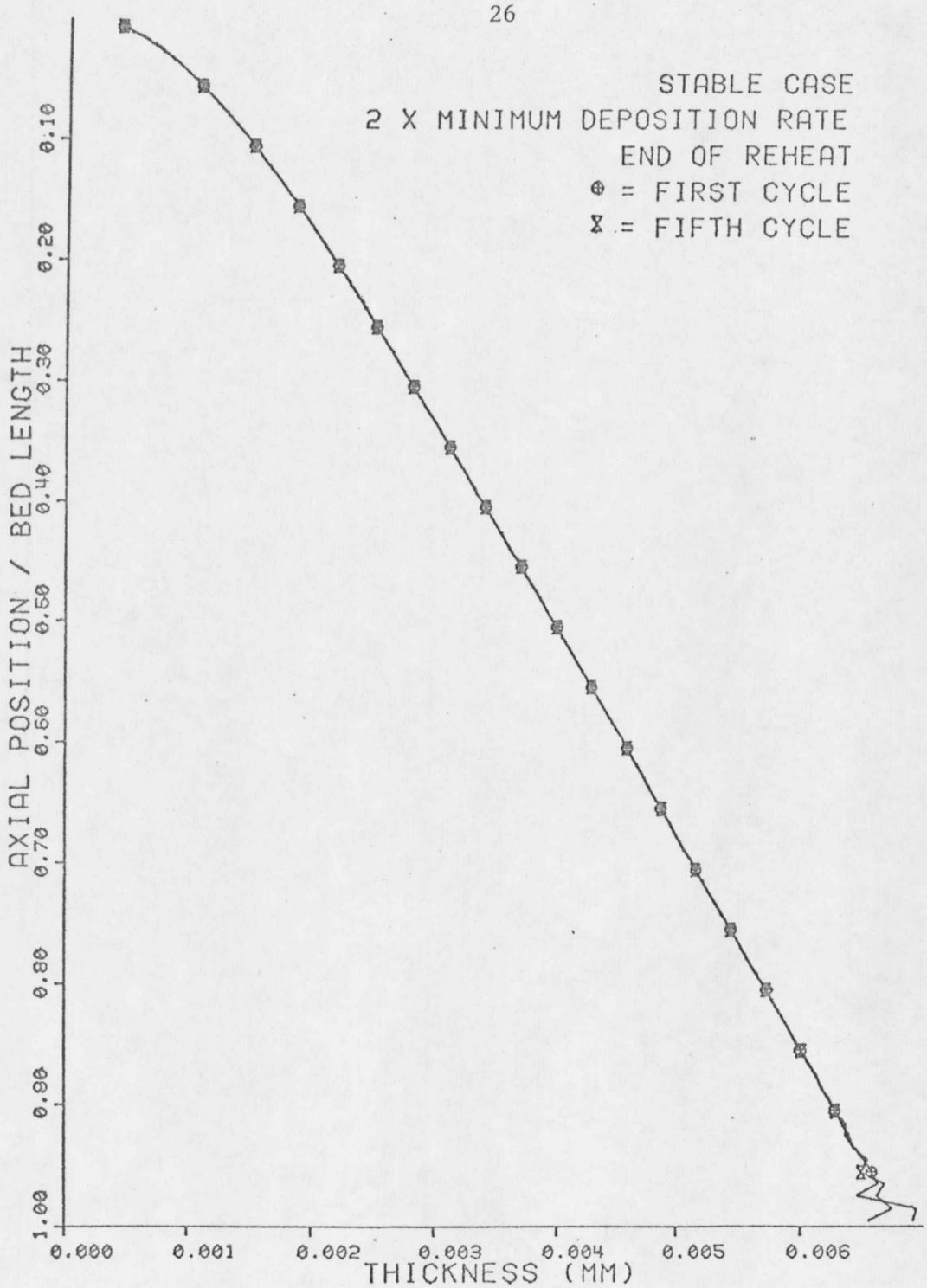

Figure 9.--Seed thickness profile

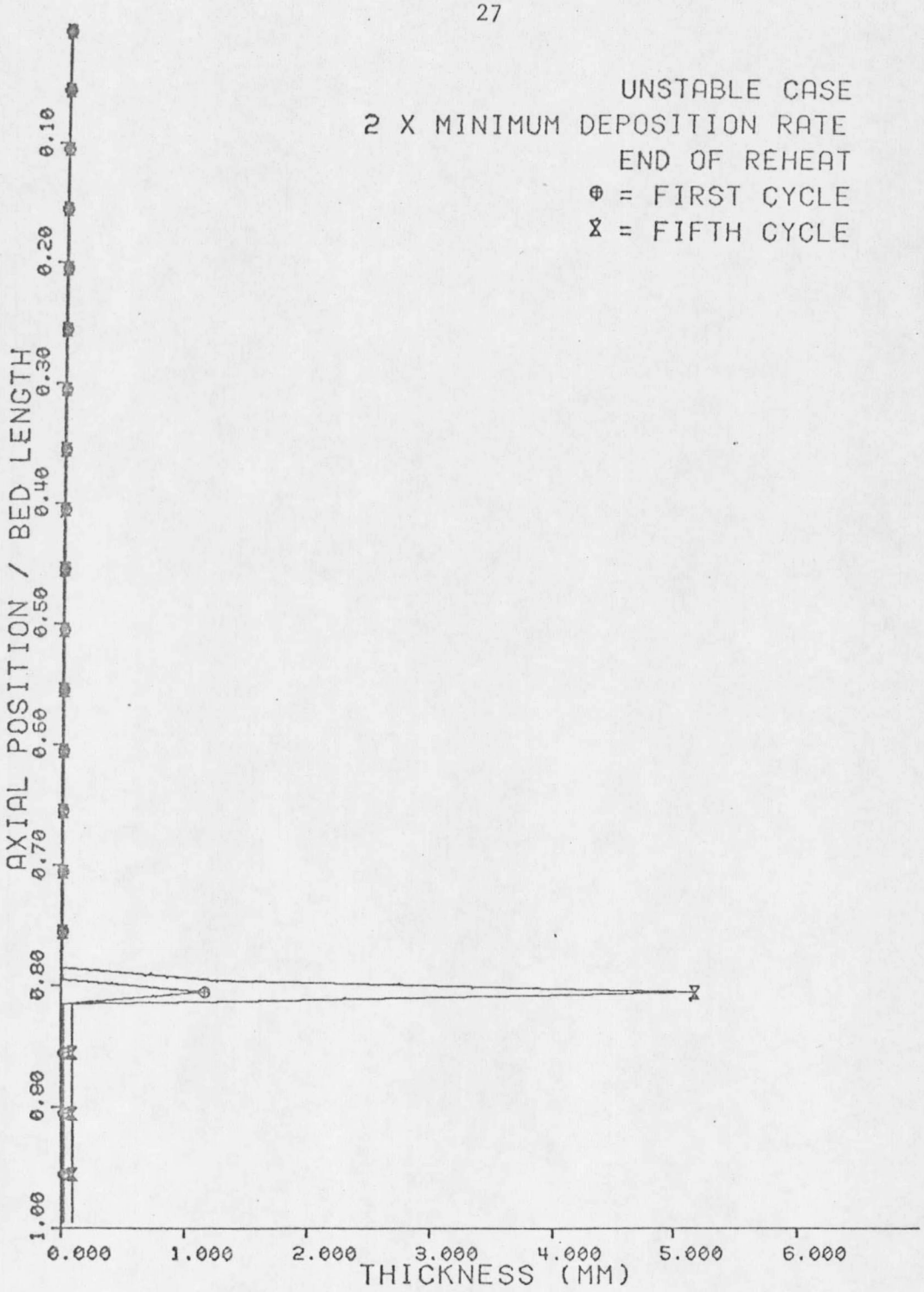

Figure 10.--Seed thickness profile

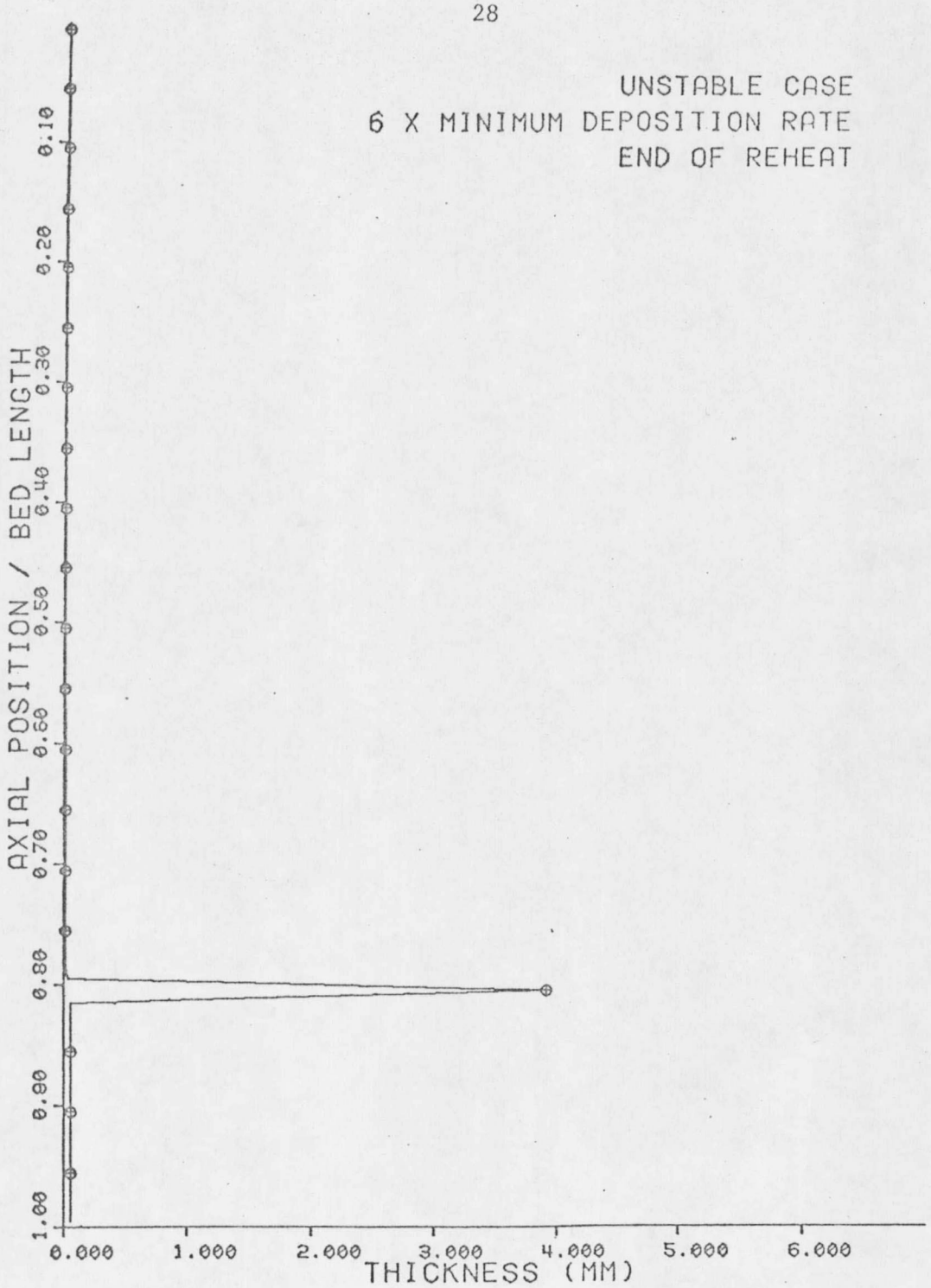

Figure 11.--Seed thickness profile

resulted in a maximum thickness of 3.9 mm. Figure 11 shows this seed thickness profile. Since the flow model predicts approximately equal growth at the point of solidification for each cycle, this last deposition rate would result in the model predicting plugging of the flow passage before five cycles are completed. Plugging did not occur in the experimental run. Therefore, it is reasonable to assume that this last deposition rate approximates the experimental value, and that the limitations of the flow model are exceeded after the first cycle. In reality, instead of having the same amount of radial growth with each cycle, the area of maximum thickness is probably experiencing considerable axial growth also, thereby slowing the radial growth. The pressure drop calculations indicate the maximum thickness should only grow approximately 1 mm radially between the first and fifth cycles of the unstable case.

Until additional refinements are made for both the analytical model and for measurement of experimental data, further comparison between the model results and experimental results are difficult to make. The analytical model does not take into account the fact that air preheater flow passages are not continuous tubes. In the experimental runs there was significant cross flow at brick interfaces as well as obvious misalignments of the bricks. This allowed varying mass flow rates along individual tube lengths. The horizontal temperature gradients in the bricks themselves resulted in the different flow passages having maximum

seed deposition at different axial positions. The total amount of seed deposited on the flow passage walls was not measurable. Neither was the rate of seed deposition measurable.

Although liquid seed drainage from the bottom of the preheater bed was an observable phenomena, no measurement of the relative rates of drainage with time was made. The analytical model indicates a surge of drainage should occur as the bottom of the bed heats to above the seed solidification temperature during the reheat phase. The analytical model also indicates the possibility of small amounts of liquid seed being blown out the top of the bed during the blowdown phase. This phenomena was not looked for during the experimental runs.

Another experimental parameter that could be helpful but is not available is the rate of change of the pressure drop across the bed. It would then be possible to compare increasing pressure drops with increasing flow restrictions to determine whether the seed thickness growth rates were reasonable. The times of occurrence of maximum pressure drops and maximum flow restrictions could also provide correlation between experimental and analytical results.

CHAPTER V

CONCLUSIONS

From the results of the two cases of seed flow modeled, it may be concluded that:

1. The analytical seed flow model can reasonably predict the occurrence of a flow restriction for known flow conditions.
2. Seed flow in an MHD air preheater will not cause a flow restriction if the entire bed length is heated to above the seed solidification temperature for a short period of time.
3. Further experimental and analytical work must be done before the behavior of large flow restrictions can be predicted.

APPENDIX 1

DEVELOPMENT OF THE PARTIAL DIFFERENTIAL EQUATION GOVERNING THE SEED LAYER THICKNESS AND RESULTING STABILITY CRITERIA

Figure 1.1 shows a single axial element of fluid in rectangular coordinates with significant flow parameters. The following mass balance can be applied to the element shown:

$$\text{mass in} - \text{mass out} = \frac{\partial}{\partial t}(\text{mass})$$

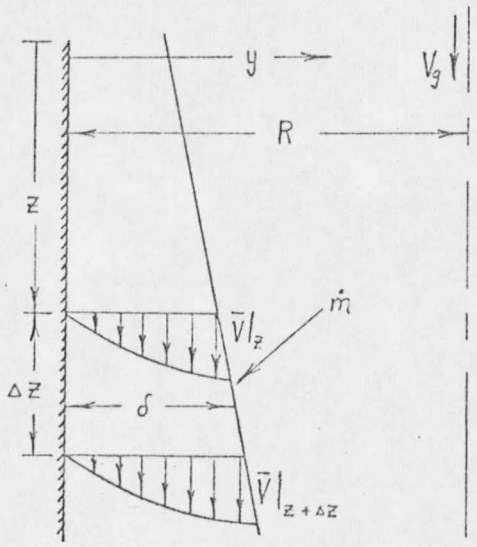

Figure 1.1 Axial Element of Fluid Layer

Expanding the terms:

$$\text{mass in} = \dot{m} \cdot C \cdot \Delta Z + \rho \cdot C \cdot \delta|_z \cdot \bar{V}|_z$$

$$\text{mass out} = \rho \cdot C \cdot \delta|_{z+\Delta z} \cdot \bar{V}|_{z+\Delta z}$$

$$\text{mass} = \rho \cdot C \cdot \delta \cdot \Delta Z$$

where: C = circumference of fluid ring, and

$\overline{V}$ = mean fluid velocity.

From the thin slag layer approximation, it can be assumed that $\delta/R \ll 1$ and therefore, the circumference of the fluid ring is a constant. Substituting the expanded terms into the mass balances gives:

$$\dot{m} \cdot C \cdot \Delta Z + \rho \cdot C \cdot \delta\big|_z \cdot \overline{V}\big|_z - \rho \cdot C \cdot \delta\big|_{z+\Delta z} \cdot \overline{V}\big|_{z+\Delta z} = \frac{\partial}{\partial t}(\rho \cdot C \cdot \delta \cdot \Delta Z)$$

Dividing through by $\rho \cdot C \cdot \Delta Z$ and applying the definition of a partial derivative results in the partial differential equation that governs the fluid thickness:

$$\frac{\dot{m}}{\rho} + \frac{\partial(\delta \cdot \overline{V})}{\partial Z} = \frac{\partial \delta}{\partial t} \qquad (1.1)$$

Equation 1.1 is a first order partial differential equation that can be easily written in any of the finite difference forms. However, for an equation such as this, there exists no standard limitation on the axial or time step sizes that will guarantee convergence or stability. Instead, any solution obtained must be tested for convergence and the stability criteria can be determined through physical reasoning applied to the particular problem being solved.

Two stability criteria were determined for this fluid flow problem. The first of these is the time step size must always be small enough that none of the axial elements is allowed to completely drain with a single step in time. This can be accomplished by calculating the time

step size required to allow a maximum percentage growth in the fluid layer before stepping in time. Should all of these calculated time steps be large enough, a single minimum time step could be used throughout the flow simulation. Otherwise, the time step size will have to be calculated prior to stepping through each time step and will vary throughout the flow simulation. The determining factor here is calculation time.

The second stability criterion is that, should the solution to the equation deviate from a smooth curve due to physical conditions, the finite difference approximation should not allow the deviation to become unbounded. The backward difference with respect to flow direction will satisfy this second criterion. That is, if the fluid is flowing downward and the axial zero position is at the top of the bed, the finite difference form of equation 1.1 is:

$$\delta_j^{n+1} = \delta_j^n + \Delta t \frac{\dot{m}_j}{\rho} + \frac{\Delta t}{\Delta Z} [\delta_{j-1}^n \cdot \bar{V}_{j-1}^n - \delta_j^n \cdot \bar{V}_j^n] \qquad (1.2)$$

where: superscript n denotes time, and

subscript j denotes axial position, measured from top of bed.

If the fluid is flowing upward and the zero axial position is at the top of the bed, the finite difference form of equation 1.1 is:

$$\delta_j^{n+1} = \delta_j^n + \Delta t \frac{\dot{m}_j}{\rho} + \frac{\Delta t}{\Delta Z} [\delta_j^n \cdot \bar{V}_j^n - \delta_{j+1}^n \cdot \bar{V}_{j+1}^n] \qquad (1.3)$$

Should the fluid change flow direction either a search routine which locates the position of the change and a combination of equations 1.2 and 1.3 will solve equation 1.1, or a more complex solution technique can be developed.

APPENDIX 2

DEVELOPMENT OF RELATIONSHIPS SIMULATING EXPERIMENTAL CONDITIONS

The following functional relationships were developed to simulate actual operating conditions for the two experimental test cases.

Temperature Functions

A graph of the axial wall temperature variations at end of blowdown and end of reheat for each test case was obtained from C. Victor Pearson [10]. Data points from this graph were used to obtain a curve fit giving temperature as a function of axial position at the end of blowdown and end of reheat for both cases. Figures 2.1 and 2.2 show the axial wall temperature profiles as determined by the developed functions. The wall temperature was assumed to vary linearly with time during reheat and during blowdown. The linear time variation was added to the axial temperature functions resulting in a reheat temperature function and a blowdown temperature function for each test case.

Stable Case

Reheat cycle:

$$\text{Temp} = 1629.8 + 212.4\,\frac{t}{RT} - 150.3Z + 22.1Z\,\frac{t}{RT} + 13.1Z^2 - 4.6Z^2\,\frac{t}{RT}$$

where: Temp = wall temperature in °K,

t = time into reheat cycle (sec),

RT = total reheat cycle time (sec), and

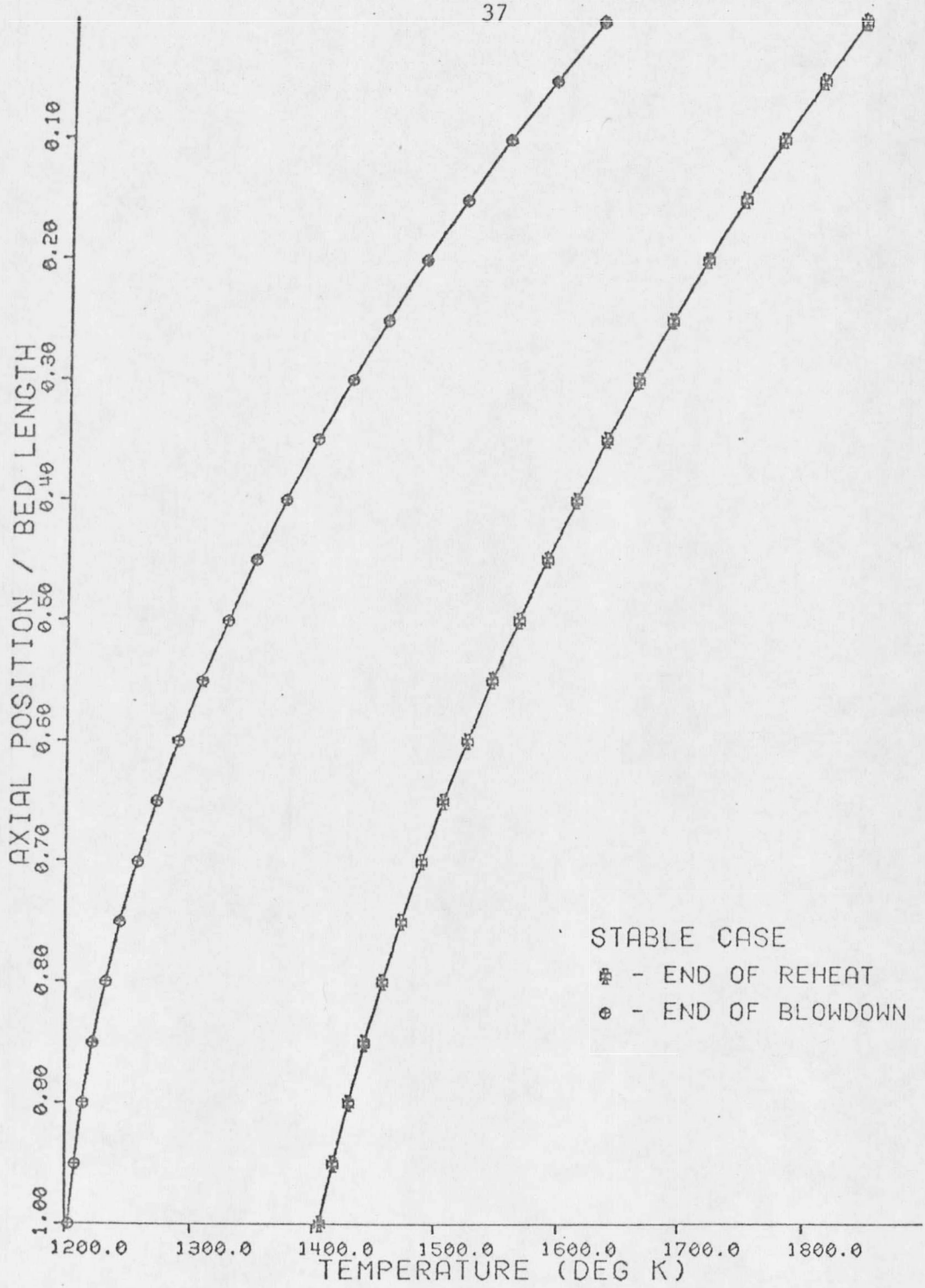

Figure 2.1.--Stable case axial temperature profiles

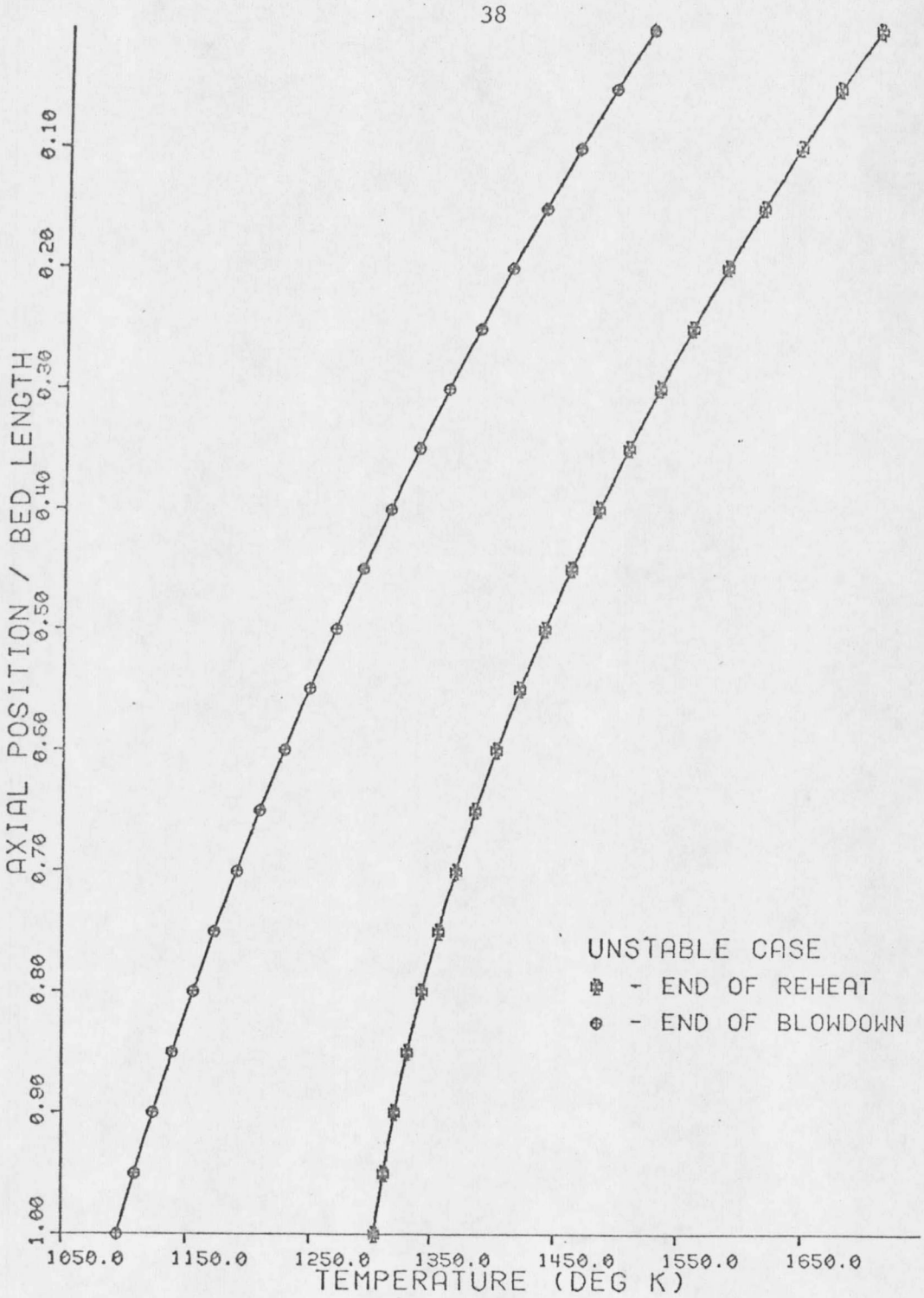

Figure 2.2.--Unstable case axial temperature profiles

Z = axial position with Z=0 at the top of the bed (m).

Blowdown cycle:

$$\text{Temp} = 1842.2 - 212.4\,\frac{t}{BT} - 128.2Z - 22.1Z\,\frac{t}{BT} + 8.5Z^2 + 4.6Z^2\,\frac{t}{BT}$$

where: t = time into blowdown cycle (sec), and

BT = total blowdown cycle time (sec).

Unstable Case

Reheat cycle:

$$\text{Temp} = 1520.9 + 185.4\,\frac{t}{RT} - 111.8Z - 15.6Z\,\frac{t}{RT} + 5.7Z^2 + 3.9Z^2\,\frac{t}{RT}$$

Blowdown cycle:

$$\text{Temp} = 1706.3 - 185.4\,\frac{t}{BT} - 127.4Z + 15.6Z\,\frac{t}{BT} + 9.6Z^2 - 3.9Z^2\,\frac{t}{BT}$$

Viscosity Function

The following empirical relationship for pure liquid potassium sulphate (K_2SO_4) viscosity as a function of temperature was obtained from Heywood and Womack [11]:

$$\mu = 10^{\left(\frac{1825}{T} - 3.96\right)}$$

$$(1273°K \leq T \leq 1673°K)$$

where: μ = viscosity in Pa·sec, and

T = temperature in °K.

The seed solidification temperature is approximately 1344°K.

Shear Functions

The following assumptions about the experimental conditions were made so that the shear functions could be developed:

1. Both the reheat gas stream and the blowdown air stream were assumed to follow the viscosity - temperature relationship given by Upshaw [12]:

$$\mu = 7.456 \times 10^{-7} \, TK^{0.5818}$$

$$(811°K \leq TK \leq 1922°K)$$

where: μ = gas stream viscosity (Pa·sec), and

TK = gas stream temperature (°K).

2. The reheat gas stream was assumed to be 55.6°K (100°F) hotter than the wall temperature.

3. The blowdown air stream was assumed to be 55.6°K (100°F) cooler than the wall temperature.

4. A square edged entrance loss was included in calculating the total pressure drop across the bed.

The 5.182 m bed was divided into 200 axial elements. Starting at the flow entrance where all the flow conditions were known and assuming the gas density to be a constant for any single axial element, the element

exit pressure, friction factor, and shear force were calculated using equations 7, 8, and 9. These calculations were repeated through the 200 elements. A trial and error procedure was used to find the value of k_s which would give a total bed pressure drop approximately equal to those measured in the stable case experiment. A k_s value of 7.62×10^{-4} m (30 mils) resulted in an end of reheat pressure drop of 6253 Pa and an end of blowdown pressure drop of 5509 Pa. This roughness factor was used in both cases and it was assumed that the higher pressure drops measured in the unstable case could be attributed to flow restrictions due to seed buildup.

Using the constant k_s value, the axial shear variation was calculated and curve fitted at end of reheat and end of blowdown conditions for both cases. The shear was assumed to vary linearly with time during reheat and blowdown.

Stable Case

Reheat cycle:

$$\tau = 5.59 + 0.74 \frac{t}{RT} - 0.468Z + 0.093Z \frac{t}{RT} + 0.0431Z^2 - 0.0161Z^2 \frac{t}{RT}$$

where: τ = shear force due to gas flow (Pa).

Blowdown cycle:

$$-\tau = 7.17 - 0.96 \frac{t}{BT} - 0.637Z + 0.047Z \frac{t}{BT} + 0.0435Z^2 + 0.0154Z^2 \frac{t}{BT}$$

Unstable Case

Reheat cycle:

$$\tau = 4.46 + 0.56\,\frac{t}{RT} - 0.294Z - 0.044Z\,\frac{t}{RT} + 0.0150Z^2 + 0.0124Z^2\,\frac{t}{RT}$$

Blowdown cycle:

$$-\tau = 3.77 - 0.46\,\frac{t}{BT} - 0.333Z + 0.049Z\,\frac{t}{BT} + 0.0253Z^2 - 0.0102Z^2\,\frac{t}{BT}$$

Mass Deposition Function

The following mass balance may be written for any axial element:

$$\dot{m}_1 = \dot{m}_d + \dot{m}_2$$

where: $\dot{m}_1$ = kg seed/sec entering axial element,

$\dot{m}_d$ = kg seed/sec deposited on wall of element, and

$\dot{m}_2$ = kg seed/sec leaving axial element.

From the stopping distance theory as shown in Ondo [6]:

$$\dot{m}_d = C_+\, k_+ \sqrt{\frac{f}{2}}\;\frac{\dot{m}_a}{A}\;\pi\, D\, \Delta Z$$

where: C_+ = weight concentration of seed in gas stream (kg seed/kg air),

k_+ = nondimensional particle deposition velocity,

f = friction factor,

$\dot{m}_a$ = mass flow rate of gas stream (kg air/sec),

A = cross sectional area of flow (m^2),

D = diameter of flow hole (m), and

ΔZ = length of axial element (m).

By definition: $\dot{m}_1 = C_{+1}\,\dot{m}_a$

$\dot{m}_2 = C_{+2}\,\dot{m}_a$

Knowing the inlet concentration and assuming it to be constant over the axial element, the exit concentration was calculated by:

$$C_{+2} = C_{+1} - \frac{\dot{m}_d}{\dot{m}_a}$$

The seed deposition rates and concentrations can be calculated segmentally as the axial elements are stepped through when k_+ is known.

For a first order approximation, the minimum Liu and Agarwal [5] measured value of k_+ that agrees closely with theoretical work as shown by Ondo [6] was used. This k_+ was 2.5×10^{-4} and it was considered to be a constant with axial position and time. The nondimensional relaxation time corresponding to this k_+ is 0.63. From Ondo, seed particle diameters of approximately 8 microns for the stable case and 9 microns for the unstable case can be determined from this nondimensional relaxation time.

LITERATURE CITED

1. Clowes, W. R., "Slag Run-Off in an MHD Air Preheater," Master of Science Thesis, Mechanical Engineering Department, Montana State University, October 1977.
2. Friedlander, S. K. and H. F. Johnstone, "Deposition of Suspended Particles from Turbulent Gas Streams," Industrial and Engineering Chemistry, Vol. 49, No. 7, July 1957.
3. Davies, C. N., Aerosol Science, Academic Press, London, 1966.
4. Sande, C. K., "The Deposition of Particulates in Turbulent Pipe Flow," Master of Science Thesis, Mechanical Engineering Department, Montana State University, December 1976.
5. Liu, B. Y. H. and J. K. Agarwal, "Experimental Observation of Aerosol Deposition in Turbulent Flow," Journal of Aerosol Science, Vol. 5, pg. 145, 1974.
6. Ondo, K., "Review of Theoretical and Experimental Small Particle Deposition in Turbulent Duct Flow," unpublished paper, Stanford University, August 1977.
7. Rosa, R. J., "Design Considerations for Coal-Fired MHD Generator Ducts," Fifth International Conference on MHD Electrical Power Generation, Munich, 1971.
8. Rodgers, M. E., P. C. Ariessohn, and C. H. Kruger, "Comparison of Measurements and Predictions of the Fluid Mechanics and Thermal Behavior of MHD Channel Slag Layers," 16th Symposium on Engineering Aspects of MHD, Pittsburgh, May 1977.

9. White, L. R., personal communication, Fluidyne Engineering Corporation, May 1978.

10. Pearson, C. V., personal communication, Argonne National Laboratory, May 1978.

11. Heywood, J. B., and G. J. Womack, Open Cycle MHD Power Generation, Pergamon Press, London, 1969.

12. Upshaw, G. A., "A Simulation Approach to the Thermal-Hydraulic Design of Cored Ceramic Brick Regenerative Heat Exchangers," Master of Science Thesis, Mechanical Engineering Department, Montana State University, June 1977.

Nash, Rosanne Marie,
Seed run-off in an
MHD air preheater